

NUMERICAL METHOD OF MULTISCALE MODELING OF THE STRESS-STRAIN STATE OF LARGE-SIZED STRUCTURES IN SITE WELDING

O.S. Milenin, O.A. Velykoivanenko, G.P. Rozyuka, N.I. Pivtorak

E.O. Paton Electric Welding Institute of the NASU
11 Kazymyr Malevych Str., 03150, Kyiv, Ukraine

ABSTRACT

A multiscale procedure was proposed for modeling the kinetics of stress-strain state of large-sized structures during site welding. This procedure is based on finite element solution of nonstationary thermoplasticity problems, characteristic for fusion welding technologies, at the mesoscale level with fine spatial breakdown of the region and with subsequent transfer of a certain amount of calculation data into a macroscopic model of a large-scale structure. Algorithms of the respective averaging of the properties and stress-strain state parameters are proposed for this purpose, which allows performing analysis of large-sized structures during welding without the need to involve significant computing power. A characteristic example of site welding of a cylindrical structure of a large diameter is used to show the applicability of the developed approach for prediction of spatial distribution of stresses and strains. Here, the most effective method is calculation of the stress fields, where a much greater sparseness of the spatial breakdown can be achieved, while calculation of the strained state is much more sensitive to finite element size.

KEYWORDS: large-sized structures, welding, stress-strain state, mathematical modeling, multiscale method, resource intensity of calculation

INTRODUCTION

Solution of the characteristic problems of optimization of the technological processes of site welding of large-sized structures is related to a number of objective difficulties because of the length of the welds, and, at the same time, local influence of welding heating. In particular, a necessary step is prediction of the current and residual stress-strain state (SSS) of the structures, which is due to the need to guarantee the admissibility of their shape change, local resistance and resistance to different types of fracture [1–3]. Experimental determination of development of the temperature, stress and strain fields in welding, in order to guarantee the proper quality of the end product, is made more complicated by material consumption of the structure and significant associated financial costs, so that application of modern methods of numerical modeling of the welding processes is rational. It allows establishing the qualitative and quantitative regularities of the influence of welding on the state of a specific structure, both at mounting, and in further operation.

Appearance of new methods of prediction of the state of large-sized structures, including those with a large number of welds, corresponds to development of understanding of physical-mechanical processes in continuous media, mathematical models, describing them, numerical methods and computer technologies. Modern principles of discrete description of

the kinetics of nonstationary multiphysical processes (primarily, by finite element methods) provide ample possibilities for solving the fundamental and applied problems. The adequacy and accuracy of the obtained numerical results depends, in particular, on the fineness of spatial breakdown, i.e. size of the finite element (FE), which is sufficient to obtain the exact solution of the necessary differential equations in the difference formulation of the problem [4]. However, as regards numerical description of the state of large-sized structures in welding, it means an excessive resource intensity of the problems, as, on the one hand, the high gradient of temperatures, stresses and strains in the welding area requires fine spatial breakdown, which cannot be used over the entire structure, and on the other hand, the great difference in FE dimensions leads to instability of the schemes of solving the respective boundary problems [5]. This caused development of simplified models, which allow describing with the required accuracy the separate technological and physical-mechanical processes in welding and related processes.

In particular, the methods of inherent strain or shrinkage functions became widely accepted for prediction of residual shape change of large-sized structures as a result of site welding [6, 7]. This class of methods involves the assumption that the residual plastic strains, caused by welding (precalculated or experimentally measured) can be assigned as the initial state of a specific structure, which is particularly

convenient in the case of presence of a large number of similar welds: in ship plating, stringer panels, etc. [8–10]. The disadvantage of the above methods is the fact that they do not allow following the current SSS of the structures during welding, but consider only the problem of the residual strained state. Moreover, in the absence of data on the kinetics of the temperature field and strained state during welding, objective difficulties arise in determination of the effective region for assigning the initial integrated or distributed plastic strains in the weld metal and HAZ. So-called 2D-X models allow modeling of the current state of large-sized structures [11], however, their applicability is quite limited. Therefore, further development of the numerical methods of prediction of the current SSS of large-sized structures during site welding is practically important, in particular, in the case of typical cylindrical pressure vessels, which is the purpose of this work.

As it was said above, one of the features of the state of large-sized structures in welding is the different scale of physical-mechanical processes in the welding area and on the periphery. This complicates the numerical realization of the respective mathematical models by the common methods, but it makes application of multilevel multiscale models rational. So, development of temperatures and SSS is of a local nature in welding, and it can be described by joint models of heat conductivity and elasto-plastic medium. For a range of cases, the local current and residual distributions of stresses and strains can be described within the simplified two-dimensional models, which allows application of small FE for their description without any significant increase of the calculation time. Transfer of a certain array of calculated data to the full three-dimensional model of a large-sized

structure with its own finite element breakdown (such, which allows conducting the respective real-time calculations) with further calculation of the general SSS is formalized by the algorithm of multiscale interconnection between the calculation levels.

So, within the scope of this work, two scale levels were considered, which are typical for the problems of prediction of the kinetics of temperature and stress-strain states of large-sized structures, namely the mezolevel, on which the welding processes are usually described, with the characteristic spatial scale of approximately 1 mm, and the macrolevel, which is characteristic for the problems of deformation of large-sized structures with the spatial scale of 1 cm and more. A finite element solution of the respective joint interrelated problems was used for a numerical description of the kinetics of the nonstationary temperature and stress-strain states in the site welding region. The respective algorithms and mathematical formulations are a development of complex approaches developed by the authors [12–14], in the context of a multiscale problem statement.

So, the kinetics of the temperature field was predicted by a numerical solution of a nonstationary heat-conductivity equation of a fast-moving heat source in the two-dimensional approximation. It allowed not only taking into account the temperature dependencies of heat conductivity and heat capacity of the structure material, but reduce as much as possible the spatial breakdown of the calculation area without any essential increase of calculation time.

Based on the calculated temperature fields in the structure cross-section at its site welding, the boundary problem of nonstationary thermoplasticity of the structure material was formulated with the respective finite element realization based on eight node FE (Figure 1). So, increment of the strain tensor can be presented in keeping with following expression:

$$d\epsilon_{ij} = d\epsilon_{ij}^e + d\epsilon_{ij}^p + \delta_{ij} d\epsilon_T, \quad (1)$$

where $d\epsilon_{ij}^e$; $d\epsilon_{ij}^p$; $\delta_{ij} d\epsilon_T$ are the components of strain tensor increase due to the elastic deformation mechanism, instant plasticity strains and kinetics of the non-uniform temperature field, respectively.

Strain increase, which is due to the kinetics of temperature T , is equal to

$$d\epsilon_T = \alpha dT, \quad (2)$$

where α is the coefficient of linear temperature expansion of the material.

The tensors of mechanical stresses σ_{ij} and elastic strains $d\epsilon_{ij}^e$ are related to each other by the generalized Hooke's law, i.e.

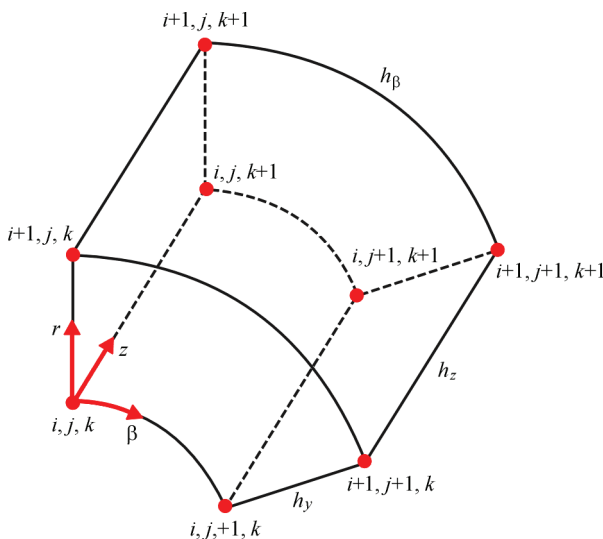


Figure 1. Scheme of an eight-node finite element in a cylindrical system of coordinates

$$\varepsilon_{ij}^e = \frac{\sigma_{ij} - \delta_{ij}\sigma}{2G} + \delta_{ij}(K\sigma + \varphi), \quad (3)$$

where $\sigma = \frac{(\sigma_{\beta\beta} + \sigma_{zz} + \sigma_{rr})}{3}$ is the mean value of normal components of stress tensor σ_{ij} , $K = \frac{1-2\nu}{E}$ is the bulk compression modulus; $G = \frac{E}{2(1+\nu)}$ is the shear modulus; E is the Young's modulus; ν is the Poisson's ratio; ν is the bulk strain.

Depending on the stressed state in a specific FE, increase of instant plasticity strains $d\varepsilon_{ij}^p$ can be calculated, using a linear dependence of scalar function Λ and deviator component of the stress tensor, namely [12]:

$$d\varepsilon_{ij}^p = d\Lambda(\sigma_{ij} - \delta_{ij}\sigma). \quad (4)$$

Quantitative value of function Λ depends on the stressed state in the considered area of the structure, as well as on the shape of material yield surface Φ , which is characterized by yield limit σ_y :

$$\begin{aligned} d\Lambda &= 0, \text{ if } \sigma_i < \sigma_y, \\ d\Lambda &> 0, \text{ if } \sigma_i = \sigma_y, \\ \sigma_i &> \sigma_y, \text{ state is inadmissible.} \end{aligned} \quad (5)$$

where $\sigma_i = \sqrt{\frac{1}{2}\sigma_{ij}\sigma_{ij}}$ is the stress intensity.

The strain tensor growth can be presented in the form of superposition of the increase of the respective components [13]:

$$\begin{aligned} \Delta\varepsilon_{ij} &= \Psi(\sigma_{ij} - \delta_{ij}\sigma) + \delta_{ij}(K\sigma + \Delta\varepsilon_y) - \\ &- \frac{1}{2G}(\sigma_{ij} - \delta_{ij}\sigma)^* - (K\sigma)^*, \end{aligned} \quad (6)$$

where δ_{ij} is the Kronecker symbol, “*” refers the respective variable to the previous tracking step; Ψ is the material state function, which determines the plastic flow condition according to Mises criterion:

$$\begin{aligned} \Psi &= \frac{1}{2G}, \text{ if } \sigma_i < \sigma_y, \\ \Psi &> \frac{1}{2G}, \text{ if } \sigma_i = \sigma_y, \\ \sigma_i &> \sigma_y, \text{ state is inadmissible.} \end{aligned} \quad (7)$$

Determination of Ψ function is performed by iteration at each step of numerical tracking (by time or by loading increase), which allows solving the non-linearity by the plastic flow of the material. Based on the specific meaning of Ψ function from (7), the strain field is determined at each loading step, taking into account $\sigma_y(T)$ dependencies:

$$\Delta\varepsilon_{ij} = \left(\Psi - \frac{1}{G}\right)(\sigma_{ij} - \delta_{ij}\sigma). \quad (8)$$

Here, at each step of iteration by Ψ , stresses σ_{ij} are calculated according to the following algorithm (summing up is performed by the repeating indices) [14]:

$$\sigma_{ij} = \frac{1}{\Psi} \left(\Delta\varepsilon_{ij} + \delta_{ij} \frac{\Psi - K}{K} \Delta\varepsilon \right) + J_{ij}, \quad (9)$$

where

$$\begin{aligned} \Delta\varepsilon &= \frac{\Delta\varepsilon_{ii}}{3}, \\ J_{ij} &= \frac{1}{\Psi} \left[(b_{ij} - \delta_{ij}b) + \delta_{ij} \left(K\sigma^* - \frac{\Delta\varepsilon_y}{K} \right) \right], \\ b &= \frac{b_{ii}}{3}, \\ b_{ii} &= \left(\frac{\sigma_{ij}}{2G} \right)^* + \delta_{ij} \left[\sigma^* \left(K - \frac{1}{2G} \right)^* - \Delta\varphi \right]. \end{aligned} \quad (10)$$

The connection between the components of strain tensor $\Delta\varepsilon_{ij}$ and displacement increment vector ΔU_i has the following mathematical expression:

$$\Delta\varepsilon_{ij} = \frac{\Delta U_{i,j} + \Delta U_{j,i}}{2}, \quad (11)$$

where the comma denotes differentiation within FE.

The stress tensor components satisfy the equations of statics for internal FE and the boundary conditions for the surface elements. In their turn, the components of $\Delta U_i = (\Delta U, \Delta V, \Delta W)$ vector meet the corresponding conditions on the boundary.

The solved system of equations in the variables of displacement increment vector in FE nodes at each step of tracking and iteration by Ψ is determined by minimizing the following functional (Lagrangian variational principle):

$$E_I = -\frac{1}{2} \sum_V (\sigma_{ij} + J_{ij}) \Delta\varepsilon_{ij} V_{m,n,r} + \sum_{S_p} P_i \Delta U_i \Delta S_p^{m,n,r}, \quad (12)$$

where \sum_V is the operator of the sum of internal FE; \sum_{S_p} is the operator of the sum of surface FE, on which the components of force vector P_i are assigned, i.e. the subsequent system of equations allows deriving the solution in the components of the displacement increment vector at each step of tracking and iteration by Ψ for a specific FE:

$$\frac{\partial E_I}{\partial \Delta U_{m,n,r}} = 0, \quad \frac{\partial E_I}{\partial \Delta V_{m,n,r}} = 0, \quad \frac{\partial E_I}{\partial \Delta W_{m,n,r}} = 0. \quad (13)$$

At consideration of cylindrical structures with a circumferential weld, the assumptions of a two-dimensional model of a plane stressed state can be used. In such a description the stress tensor σ_{ij} ($i, j = r, \beta, z$) includes four nonzero components $\sigma_{rr}, \sigma_{zz}, \sigma_{\beta\beta}, \sigma_{rz}$. Strain increase tensor $\Delta\varepsilon_{ij}$ contains similar nonzero components. The components of this tensor are connected with the components of displacement increase ΔU_r and ΔU_z by the following relationships:

$$\begin{aligned} \Delta\varepsilon_{rr} &= \frac{\partial\Delta U_r}{\partial r}, \quad \Delta\varepsilon_{zz} = \frac{\partial\Delta U_z}{\partial z}, \\ \Delta\varepsilon_{rz} &= \frac{1}{2} \left(\frac{\partial\Delta U_r}{\partial z} + \frac{\partial\Delta U_z}{\partial r} \right), \quad \Delta\varepsilon_{\beta\beta} = \frac{\Delta U_r}{r}. \end{aligned} \quad (14)$$

The connection between σ_{ij} and $\Delta\varepsilon_{ij}$ can be described as follows:

$$\begin{aligned} \sigma_{rr} &= A_1 \Delta\varepsilon_{rr} + A_2 (\Delta\varepsilon_{\beta\beta} + \Delta\varepsilon_{zz}) + Y_{rr}, \\ \sigma_{\beta\beta} &= A_1 \Delta\varepsilon_{\beta\beta} + A_2 (\Delta\varepsilon_{rr} + \Delta\varepsilon_{zz}) + Y_{\beta\beta}, \\ \sigma_{zz} &= A_1 \Delta\varepsilon_{zz} + A_2 (\Delta\varepsilon_{rr} + \Delta\varepsilon_{\beta\beta}) + Y_{zz}, \\ \sigma_{rz} &= A_3 \Delta\varepsilon_{rz} + Y_{rz}, \end{aligned} \quad (15)$$

where

$$\begin{aligned} A_1 &= \frac{\Psi + 2K}{3K\Psi}, \quad A_3 = \frac{1}{\Psi}, \quad A_2 = A_1 - A_3 = \frac{\Psi - K}{3K\Psi}, \\ Y_{ij} &= \frac{1}{\Psi} \left(\frac{\sigma_{ij} - \delta_{ij}\sigma}{2G} \right)^* + \delta_{ij} \frac{(K\sigma)^* - \Delta\varphi}{K}. \end{aligned} \quad (16)$$

Equations (15), (16) form a system of linear algebraic equations for strains (displacements), which is the base of finite element realization of the numerical solution.

As noted above, application of a similar approach for description of the temperature state, current and residual SSS of a large-sized structure based on fine spatial breakdown is complicated or impossible, because of an excess resource consumption of such a problem. However, increase of the steps of spatial breakdown in the macroscale approach can lead to a loss of accuracy of the calculation model right up to a significant distortion of the results. Therefore, the results obtained in keeping with the mesoscale calculation were used as the initial data for macroscale calculation, but taking into account the integral interpretation required for it. That is, in order to track the state of one FE of the macroscopic problem it is necessary to use an averaged state of several FE of the mezoproblem during the entire technological cycle of site welding. The result of such averaging should be the integral values of mechanical properties of the material of a nonuniformly heated structure and parameters of its current deformed state. So, a simplified approach can be used for averaging the material mechanical properties, namely Young's modulus, the

coefficient of linear thermal expansion and yield limit, similar to the rule of mixtures. This is substantiated by the characteristically small gradients of properties at distances of the order of FE size, that is necessary for a stable solution of the boundary problem of nonstationary thermoplasticity in the definition of (1)–(13). Therefore, if the state of mn element in the macroproblem is described by several elements ij in the mesoscale definition, the respective mechanical characteristics can be evaluated as follows:

$$E'_{mn} = \frac{\sum_i \sum_j E(T_{ij}) s_{ij}}{\sum_i \sum_j s_{ij}}, \quad \alpha'_{mn} = \frac{\sum_i \sum_j \alpha(T_{ij}) s_{ij}}{\sum_i \sum_j s_{ij}}, \quad (17)$$

where s_{ij} is the area of ij -th FE; T_{ij} is the temperature in ij point; “'” refers the parameter to the macroproblem.

It should be noted that relationship (17) was formulated in a two-dimensional definition, but averaging from a two-dimensional to a three-dimensional problem can be realized similarly.

Development of SSS in a macroscopic definition requires allowing for the force factor, namely nonuniform deformation of the material. In order to calculate the distribution of the current and residual SSS, which satisfies the condition of equilibrium (13) and does not get any significant distortion on coarse spatial grids, the following spatial averaging was proposed for the numerical components of the matrix (15)–(16) and material state function Ψ , defined according to (7):

$$\begin{aligned} A'_{kmn} &= \frac{\sum_i \sum_j A_{k\ mn} s_{ij}}{\sum_i \sum_j s_{ij}}, \quad k = 1, 2, 3; \\ Y'_{mn} &= \frac{\sum_i \sum_j Y_{ij} s_{ij}}{\sum_i \sum_j s_{ij}}; \quad \Psi'_{mn} = \frac{\sum_i \sum_j \Psi_{ij} s_{ij}}{\sum_i \sum_j s_{ij}}. \end{aligned} \quad (18)$$

Solution of the system of linear algebraic equations (15) in the framework of formulation of a macroscopic problem of SSS allows obtaining equilibrium distributions of the structure stress and strain fields at each tracking step.

The limits of applicability and features of the developed multiscale approach were studied on the characteristic example of site welding of circumferential joints of a cylindrical structure from AMg6 aluminium alloy ($E = 71$ GPa, $\nu = 0.3$, $\sigma_y = 170$ MPa, $\alpha = 2.26 \cdot 10^{-5}$ $1/^\circ\text{C}$ at 20°C) of diameter $D = 3900$ mm and with wall thickness $t = 10$ mm; welding was performed in the following mode: $U = 20$ V, $I = 380$ A,

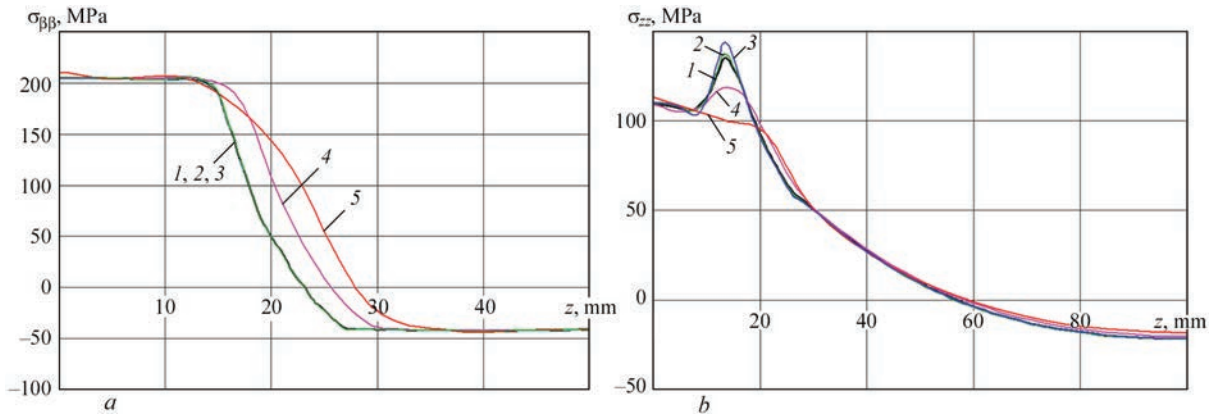


Figure 2. Calculated distribution of residual postweld circumferential $\sigma_{\beta\beta}$ (a) and axial σ_{zz} (b) stresses: 1 — control 3D calculation at $h_r = h_z = h_\beta = 1$ mm; 2 — multiscale calculation at $h_r = 4$ mm; $h_z = h_\beta = 1$ mm; 3 — multiscale calculation at $h_r = 8$ mm, $h_z = h_\beta = 1$ mm; 4 — multiscale calculation at $h_z = 4$ mm, $h_r = h_\beta = 1$ mm 5 — multiscale calculation at $h_z = 8$ mm; $h_r = h_\beta = 1$ mm (in Figure 2, a, curves 1, 2 and 3 practically coincide)

$v_w = 2.23$ mm/s. It should be noted that selection of the studied structure corresponds to the typical structural solutions for space applications, in particular, rocket-carrier fuel tanks, although the versatility of the proposed approach allows consideration of a wide range of materials, structural elements and welding technologies.

The mesoscale definition was realized within the joint solution of the problem of temperature field kinetics in welding and development of an elastoplastic deformed and stressed states of the structure in the area of the joint in the two-dimensional definition, which allowed application of fine and regular spatial finite element breakdown with the linear size of the element $h_r = h_z = 1$ mm in the radial and axial directions. At formulation of the three-dimensional problem the linear size of finite elements in the radial and axial directions was multiplied by 2, 4 and 8 times, and the stress and strain fields, obtained within the multiscale formulation of the problem and direct three-dimensional modeling with spatial step $h_r = h_z = h_\beta = 1$ mm, were compared.

As shown in Figure 2, comparisons of the calculated distributions of circumferential $\sigma_{\beta\beta}$ and axial σ_{zz} stresses for different macroscale spatial breakdown confirm the high degree of correspondence of the results of multiscale modeling to direct calculations. Significant differences appear, when the characteristic spatial distribution of local stresses becomes smaller than one step of the macroscale problem, where the respective averaging takes place (in particular, at h_z increase up to 8 mm). Here, in other structure areas, where the residual stress gradient is less significant, the correspondence of the calculations by two approaches is high (error of less than 2 %). Such an accuracy of the multiscale approach is related to the physical essence of mathematical formulation (18), namely transfer of the averaged internal energy of

the deformed material. It allows application of the proposed procedure for analysis of the stressed state of large-sized welded structures, in particular under the impact of complex operational load, as well as for brittle strength analysis. It should be noted that the maximum value of residual stresses is somewhat higher than the room temperature material yield limit. It is attributable to the fact that the cylindrical structure is characterized by a two-axial stressed state, so that the stress intensity value σ_i is somewhat lower than some individual components of the stress tensor, but σ_i itself determines the material flow surface Φ , in keeping with the Mises yield condition, in particular in the form of (5).

Similar calculations of strain field kinetics showed that the influence of multiscale approach on the error of the results of prediction of the residual deformed state is significantly higher (Figure 3). So, increase of h_r within the selected range only slightly influences the calculated value of circumferential strains $\varepsilon_{\beta\beta}$ (the error is equal to approximately 1.7 %), whereas for longitudinal strains ε_{zz} the satisfactory result of multiscale modeling is observed for a slight increase of spatial breakdown (two times up to 2 mm size). The conclusion about the relatively low possibilities for h_z increase is similar: rarefaction of spatial breakdown up to 4 times allows obtaining a satisfactory value of multiscale prediction error $\varepsilon_{\beta\beta}$ (error of less than 7 %), while for obtaining correct results for ε_{zz} , h_z increase should not be greater than 2 times up to 2 mm size.

Such analysis results are explained by that one of the main assumptions of finite element modeling is the uniformity of properties of each of the FE. A significant increase of element size leads to incorrect definition of the problem, which is manifested, primarily, in the strain field not corresponding to the true solution on fine meshes. This instability, however, corresponds, first of all to the deformed state in the

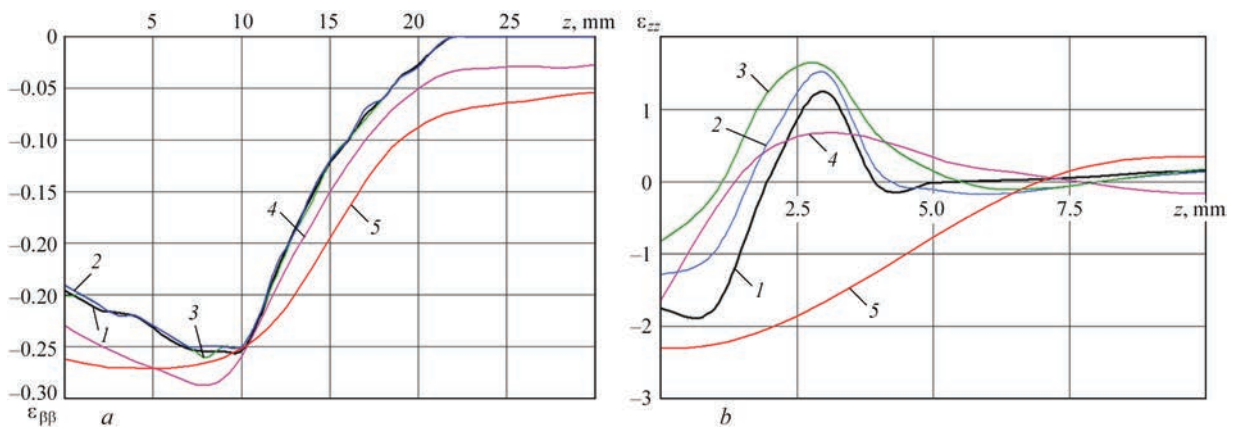


Figure 3. Calculated distribution of residual postweld circumferential $\varepsilon_{\beta\beta}$ (a) and axial ε_{zz} (b) strains (see Figure 2 for description of curves 1–5)

axial direction, where the maximum strain gradient is observed, whereas for $\varepsilon_{\beta\beta}$ and stressed state the possibilities for optimization of calculations for large-sized structures by application of the proposed multiscale approach are much higher.

As shown by calculations, simultaneous increase of spatial steps in the radial and axial directions only slightly changes the made conclusions, as the instability of individual solutions as a result of rarefaction in the axial direction prevails.

Despite the fact that in this work a concrete case of a welded large-sized structure from an aluminium alloy was considered, the derived results are sufficiently general to enable a wider application of the developed procedure and general recommendations for the cases of structures from other materials, of different geometrical dimensions, or those manufactured with application of other technologies or modes of site welding. A fundamental difference will be in the current and residual stress and strain gradients, which will determine the admissible linear averaging size (17), (18). For instance, reduction of the HAZ (at application of smaller heat input or at lower heat conductivity of the material of the large-sized structure) will determine the proportionally smaller size of spatial breakdown of the macroscopic problem in the welding area, but larger on the periphery, where the respective stress and strain gradients will be significantly smaller.

CONCLUSIONS

1. In order to develop efficient methods of analysis of the technological processes of welding without any significant increase of resource intensity of the respective calculations, a multiscale approach of numerical prediction of the kinetics of temperatures and stress-strain state was proposed. This procedure is based on finite element solution of the problems of nonstationary thermoplasticity, characteristic for fusion welding technologies, on the mesoscale level with fine spatial breakdown of the structure in a two-dimensional defi-

nition with subsequent transfer of a certain volume of the calculation data into a three-dimensional macroscopic model with a sparse mesh. For this purpose, the algorithms of the respective averaging of the properties and parameters of the stressed-strained state were proposed, which allows conducting analysis of the state of large-sized structures during welding without the need to involve considerable computing power.

2. The high correspondence of the results of finite element calculations of the stressed state within the developed model and control calculations by standard approaches was demonstrated in the case of site welding of a circumferential weld of a large-sized pressure vessel from AMg6 aluminium alloy. It is shown that a significant increase (up to eight times) of spatial finite element breakdown is possible, until the characteristic spatial breakdown of local stresses becomes smaller than one step of the macroscale problem, where the respective averaging takes place.

3. It is shown that the possibilities of application of the proposed approach for prediction of the deformed state of large-sized structures are limited as a result of shrinkage processes at nonuniform heating in welding. This is due to high calculated strain gradients, particularly in the axial direction. In such a case, spatial averaging of the properties of the material of the structure being welded, may lead to convergence of the problem within the finite element definition, and to a wrong solution.

REFERENCES

1. Deng, D., Murakawa, H., Liang, W. (2007) Numerical simulation of welding distortion in large structures. *Comput. Methods Appl. Mech. Engrg.*, **196**, 4613–4627. DOI: <http://dx.doi.org/10.1016/j.cma.2007.05.023>
2. Park, J.-U., An, G., Woo, W. et al. (2014) Residual stress measurement in an extra thick multi-pass weld using initial stress integrated inherent strain method. *Marine Structures*, **39**, 424–437. DOI: <http://dx.doi.org/10.1016/j.marstruc.2014.10.002>
3. Zhang, L., Michaleris, P., Marugabandhu, P. (2007) Evaluation of applied plastic strain methods for welding distortion

- prediction. *J. of Manufacturing Sci. and Eng.*, **129**, 1000–1010. DOI: <http://dx.doi.org/10.1115/1.2716740>
4. Liu, R.-F., Wang, J.-C. (2022) Application of finite element method to effect of weld overlay residual stress on probability of piping failure. *Inter. J. of Pressure Vessels and Piping*, **200**, 104812. DOI: <https://doi.org/10.1016/j.ijpvp.2022.104812>
 5. Li, S., Coraddu, A., Oneto, L. (2022) Computationally aware estimation of ultimate strength reduction of stiffened panels caused by welding residual stress: From finite element to data-driven methods. *Engineering Structures*, **264**, 114423. DOI: <https://doi.org/10.1016/j.engstruct.2022.114423>
 6. Bayraktar, C., Demir, E. (2022) A thermomechanical finite element model and its comparison to inherent strain method for powder-bed fusion process. *Additive Manufacturing*, **54**, 102708. DOI: <https://doi.org/10.1016/j.addma.2022.102708>
 7. Takezawa, A., To, A.C., Chen, Q. et al. (2020) Sensitivity analysis and lattice density optimization for sequential inherent strain method used in additive manufacturing process. *Computer Methods in Applied Mechanics and Engineering*, **370**, 113231. DOI: <https://doi.org/10.1016/j.cma.2020.113231>
 8. Liangfeng, L., Cheng, L., Jie, S., Yansong, Z. (2022) Numerical prediction of welding deformation in ship block subassemblies via the inhomogeneous inherent strain method. *J. of Manufacturing Processes*, **80**, 860–873. DOI: <https://doi.org/10.1016/j.jmapro.2022.06.044>
 9. Honaryar, A., Iranmanesh, M., Liu, P., Honaryar, A. (2020) Numerical and experimental investigations of outside corner joints welding deformation of an aluminum autonomous catamaran vehicle by inherent strain/deformation FE analysis. *Ocean Engineering*, **200**, 106976. DOI: <https://doi.org/10.1016/j.oceaneng.2020.106976>
 10. Makhnenko, O.V., Muzhichenko, A.F., Seyffarth, P. (2009) Application of mathematical modelling in thermal straightening of shipbuilding panels. *Paton Welding J.*, **1**, 6–11.
 11. Makhnenko, V.I., Milenin, A.S., Semyonov, A.P. (2007) Mathematical modelling of thermal-deformation processes in braze-welding of butt joints of the titanium-aluminium type. *Paton Welding J.*, **11**, 5–9.
 12. Makhnenko, V.I., Pochinok, V.E. (2006) *Strength calculation of welded joints with crack-like imperfections*. PWI, NASU.
 13. Makhnenko, V.I. (2006) *Safe service life of welded joints and assemblies of modern structures*. Kyiv, Naukova Dumka [in Russian].
 14. Velikoivanenko, E., Milenin, A., Popov, A. et al. (2019) Methods of numerical forecasting of the working performance of welded structures on computers of hybrid architecture. *Cybernetics and Systems Analysis*, **55(1)**, 117–127. DOI: <https://doi.org/10.1007/s10559-019-00117-8>

ORCID

O.S. Milenin: 0000-0002-9465-7710

CONFLICT OF INTEREST

The Authors declare no conflict of interest

CORRESPONDING AUTHOR

O.S. Milenin

E.O. Paton Electric Welding Institute of the NASU
11 Kazymyr Malevych Str., 03150, Kyiv, Ukraine.E-mail: asmilenin@ukr.net**SUGGESTED CITATION**O.S. Milenin, O.A. Velykoivanenko, G.P. Rozyuka, N.I. Pivtorak (2023) Numerical method of multiscale modeling of the stress-strain state of large-sized structures in site welding. *The Paton Welding J.*, **4**, 21–27.**JOURNAL HOME PAGE**<https://patonpublishinghouse.com/eng/journals/tpwj>

Received: 03.04.2023

Accepted: 25.05.2023

XXI INTERNATIONAL INDUSTRIAL FORUM - 2023

INTERNATIONAL TRADE FAIRS

METALWORKING
UKRWELDING
HYDRAULICS, PNEUMATICS
BEARINGS
UKRUSEDTECH
UKRFOUNDRY
AUTOMATION AND ROBOTICS
PATTERNS, STANDARDS AND INSTRUMENTS
INDUSTRIAL SAFETY
HOISTING AND TRANSPORTING, STOREHOUSE EQUIPMENT



ufi
Approved Event

30 – 01

MAY JUNE

General Information Partner:



INTERNATIONAL EXHIBITION CENTRE
15 Brovarskyi Ave., Kyiv, Ukraine
"Livoberezhna" Metro station
☎ +38 (095) 268 05 87, (84)
✉ is@iec-expo.com.ua,
helen@iec-expo.com.ua
🌐 www.iec-expo.com.ua